

H-mode fueling optimization with the supersonic deuterium jet in NSTX

V. A. Soukhanovskii¹, M. G. Bell², R. E. Bell², D. A. Gates²,
 R. Kaita², H. W. Kugel², B. P. LeBlanc², D. P. Lundberg², R. Maingi³, J. E. Menard²,
 R. Raman⁴, A. L. Roquemore², D. P. Stotler²

¹ Lawrence Livermore National Laboratory, Livermore, CA, USA

² Princeton Plasma Physics Laboratory, Princeton, NJ, USA

³ Oak Ridge National Laboratory, Oak Ridge, TN, USA

⁴ University of Washington, Seattle, WA, USA

Introduction High-performance, long-pulse 0.7-1.2 MA 6-7 MW NBI-heated small-ELM H-mode plasma discharges are developed in the National Spherical Torus Experiment (NSTX) as prototypes for confinement and current drive extrapolations to future spherical tori [1]. It is envisioned that innovative lithium coating techniques [2, 3] for H-mode density pumping and a supersonic deuterium jet for plasma refueling will be used to achieve the low pedestal collisionality and low n_e/n_G fractions (0.3-0.6), both of which being essential conditions for maximizing the non-inductive (bootstrap and beam driven) current fractions.

The low field side supersonic gas injector (SGI) on NSTX consists of a small converging-diverging graphite Laval nozzle and a piezoelectric gas valve. The nozzle is capable of producing a deuterium jet with Mach number $M \leq 4$, estimated gas density at the nozzle exit $n \leq 5 \times 10^{23} \text{ m}^{-3}$, estimated temperature $T \geq 70 \text{ K}$, and flow velocity $v = 2.4 \text{ km/s}$. The nozzle Reynolds number $Re_{is} \simeq 6000$. The nozzle and the valve are enclosed in a protective carbon fiber composite shroud and mounted on a movable probe at a midplane port location [4, 5].

Despite the beneficial L-mode fueling experience with supersonic jets in limiter tokamaks [6, 7], there is a limited experience with fueling of high-performance H-mode divertor discharges [8] and the associated density, MHD stability, and MARFE limits. In initial supersonic deuterium jet fueling experiments in NSTX, a reliable H-mode access, a low NBI power threshold, $P_{LH} \leq 2 \text{ MW}$, and a high fueling efficiency (0.1-0.4) have been demonstrated [9, 10]. Progress has also been made toward a better control of the injected fueling gas by decreasing the uncontrolled high field side (HFS) injector fueling rate by up to 95 % and complementing it with the supersonic jet fueling.

These results motivated recent upgrades to the SGI gas delivery and control systems. The new SGI-Upgrade (SGI-U) capabilities include multi-pulse ms-scale controls and a reservoir gas pressure up to $P_0 = 5000 \text{ Torr}$ [11]. In this paper we summarize recent progress toward optimization of H-mode fueling in NSTX using the SGI-U.

Results The radial propagation of a high-pressure D_2 jet through the edge plasma is determined by the radial fluid force balance from the relative magnitude of the plasma magnetic and kinetic pressures and the gas jet pressure. The high-pressure jet undergoes molecular and atomic reactions as it propagates through the scrape-off layer (SOL), retaining a neutral core shielded by an ionizing layer. The gas jet density plays a critical role in the penetration mechanism [8, 12, 13]. However, a high density region that develops in front of the low field side jet may inhibit a deep penetration.

The increased plenum pressure range in SGI-U led to a higher flow rate, up to 10^{22} s^{-1} , and a greater fueling flexibility.

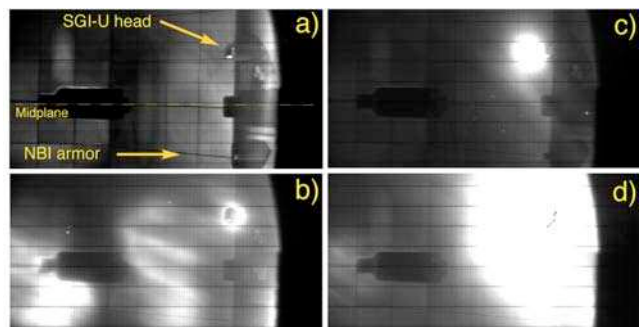


Figure 1: Fast camera images of jet-plasma interaction: (a) SGI-U head in the vacuum vessel at $R = 1.57 \text{ m}$, (b) Plasma interaction with SGI-U head during an MHD event, (c) D_α emission from jet in the initial phase of high-pressure injection, (d) D_α emission during high-pressure injection.

Before the upgrade, the SGI jet impact pressure was limited to about 30 kPa at the nozzle exit, and about 0.02 kPa at a distance 10 cm from the nozzle [9]. The jet impact pressure in the SGI-U at $P_0 = 4100$ Torr was measured to be about 5 times higher [11]. The plasma pressure at the separatrix was in the range $P = P_{kin} + P_{magn} \simeq 0.01 - 0.1$ kPa, suggesting that the SGI-U jet might be able to penetrate closer to the separatrix.

Fast framing camera images taken during SGI-U operation showed a highly localized plasma-jet interaction (Fig. 1). A bright localized D_α light region was consistent with the measured jet divergence half-angle of $\theta = 6 - 25^\circ$. The size of the D_α light-emitting region was 5-10 cm, typically much smaller than the light-emitting cloud from a conventional gas injector (GI). The light-emitting region (plasmoid) was typically elongated along the field line and shifted in the ion diamagnetic drift direction. The plasmoid was located at 0.5 - 6.0 cm outside of the separatrix, suggesting that the ionization source was also located in the SOL.

Fueling efficiency and deposition characteristics of the supersonic D_2 jet were inferred from the spatially resolved electron density measurements. Shown in Fig. 2 are the waveforms of a 4-6 MW NBI-heated H-mode discharge fueled by a HFS injector at a reduced average rate $\Gamma_{HFS} \simeq 8.5 \times 10^{20} \text{ s}^{-1}$ and the SGI-U operated at $\Gamma_{SGI-U} \simeq 8.4 \times 10^{21} \text{ s}^{-1}$. The SGI-U was located at $R = 1.57$ m, within 5-10 cm from the separatrix. The H-mode transition occurred at 0.26 s, so the first SGI-U pulse was injected in the L-mode, while two subsequent pulses were in the H-mode phase. The SOL density did not change during the SGI-U injection. The inboard and outboard pedestal density increased, suggesting that particles were deposited in the edge/pedestal region. The total electron inventory $N_e(t) = \int n_e dV$ also increased during the SGI-U pulses as evident from its time derivative dN_e/dt . However, the edge particle confinement time appeared to be low ($\tau \leq 10 - 20$ ms), and the deposited particles were eventually lost from the pedestal plasma. The plasma T_e, n_e profiles shown in Fig. 2 indicated that a SGI-U pulse in the H-mode phase led to a rapid increase in the pedestal density by 10-30 %, and a small pedestal temperature decrease. The gas jet fueling efficiency $\eta = (d \Delta N_e / dt) \Gamma_{SGI}^{-1}$ estimated from the total electron inventory N_e derivative and the SGI-U injection rate, was in the range 0.1 - 0.3. It was comparable to the SGI fueling efficiency obtained at lower plenum pressures.

Previous work on H-mode fueling optimization in NSTX resulted in the HFS fueling scenario [14]. However, the uncontrolled HFS gas injection led to continuous fueling, detachment of the inner divertor leg at low density $\bar{n}_e \simeq (2 - 3) \times 10^{19} \text{ m}^{-3}$ [15], and the inner divertor MARFE formation, thought to be responsible for the monotonic density rise observed in most NBI-heated ELM-free or small ELM H-mode discharges. To achieve better density control, H-mode experiments were carried out with the reduced HFS fueling complemented by the SGI-U.

Shown in Fig. 3 are the waveforms of three 0.8 MA, 4-6 MW NBI-heated ELM-free H-mode discharges, fueled by various D_2 quantities from the HFS and SGI-U injectors. Three cases are shown: 1) HFS fueling at $\Gamma_{HFS} \simeq 2.8 \times 10^{21} \text{ s}^{-1}$, no SGI-U; 2) reduced HFS fueling at $\Gamma_{HFS} \simeq 8.5 \times 10^{20} \text{ s}^{-1}$, three SGI-U pulses at $\Gamma_{SGI-U} \simeq 8.4 \times 10^{21} \text{ s}^{-1}$ (same discharge shown in Fig. 2); and 3) reduced HFS fueling at $\Gamma_{HFS} \simeq 6 \times 10^{20} \text{ s}^{-1}$, one SGI-U pulse. Evident from the figure is a significant, 30-50 % line-averaged density reduction due to the reduced HFS injector rate.

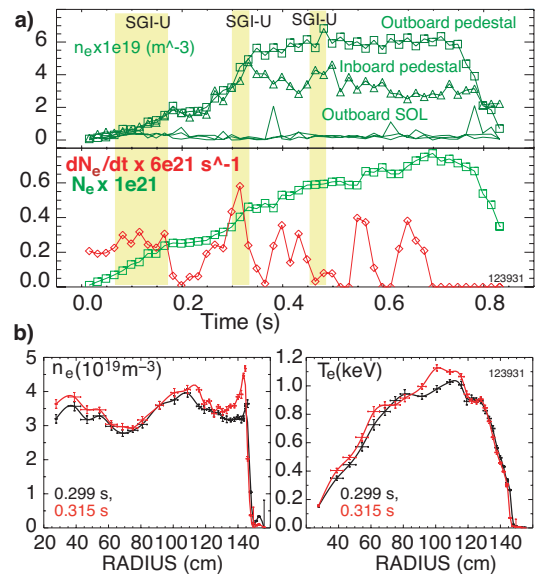


Figure 2: (a) Density waveforms of an H-mode discharge, with SGI-U injection shown by yellow bars; (b) n_e, T_e profiles just before and during the SGI-U pulse at 0.3 s.

A clear density increase due to SGI-U fueling is evident in the H-mode phase when the cases 2) and 3) are compared. Divertor D_α traces indicated that the HFS injection created a constant elevated recycling background. The particles injected by the SGI-U caused a prompt build-up in the divertor recycling, which decayed to the background level after the pulse. The outer midplane neutral pressure measured by a micro-ion gauge appeared to be sensitive to the HFS rate, and only weakly sensitive to the SGI-U injection. The inner divertor pressure, measured by the divertor Penning gauge, followed the divertor D_α trend - it was proportional to the HFS rate, and promptly responded to the SGI-U pulses. The observations suggest that there is a strong link between the SGI-U fueling and divertor recycling. While little gas from SGI-U is spread throughout the vacuum vessel, the injected particles are deposited in the H-mode pedestal by radial plasma transport and then recycled in the divertor, building up the divertor neutral pressure and contributing to the density rise.

The increased recycling in the divertor may lead to undesirable effects such as an X-point MARFE and confinement degradation. Distinctive features of the MARFE are low T_e , high n_e , and a greatly increased electron-ion recombination rate R_{rec} . Deuterium high- n series emission lines are indicative of such conditions [16]. Spatially resolved divertor profiles, obtained recently with a 10-channel divertor spectrometer, provided evidence that an X-point MARFE formed during the SGI-U pulse. Shown in Fig. 4 is a time history of the divertor Stark-broadened Balmer B10 line profile, proportional to both n_e and R_{rec} . The appearance of the X-point MARFE was closely correlated with the SGI-U pulse, and led in this case to a weak confinement degradation. Further measurements are planned to elucidate on the formation and migration mechanisms of the SGI-U-induced X-point MARFEs.

Integrated modeling of the high-pressure supersonic jet interaction with a magnetized plasma is a complex process, as the model must include a self-consistent treatment of the neutral, ion, electron, and photon fluids, as well as atomic and molecular physics effects, including molecular clustering. However, if a lower pressure SGI is not in the self-shielding regime, a single-particle tracking Monte Carlo neutral transport model may provide insights on jet penetration mechanism. We have performed a comparative modeling of the SGI and conventional GI using the DEGAS 2 code [17]. Calculations were performed on a mesh generated from a H-mode equilibrium of an SGI-fueled discharge. Measured plasma background T_e and n_e profiles were used. A Maxwellian velocity distribution corresponding to a gas temperature of $T = 160$ K with a shift of $v = 2.4$ km/s was prescribed to the supersonic gas jet. Room temperature deuterium ($T = 300$ K) was used for the thermal GI. The SGI and GI fueling efficiencies η were found to be comparable, being in the range 0.35-0.39 for H-mode plasmas. In the simulations, the SGI molecular and ion source appeared to be highly localized. In contrast, a larger

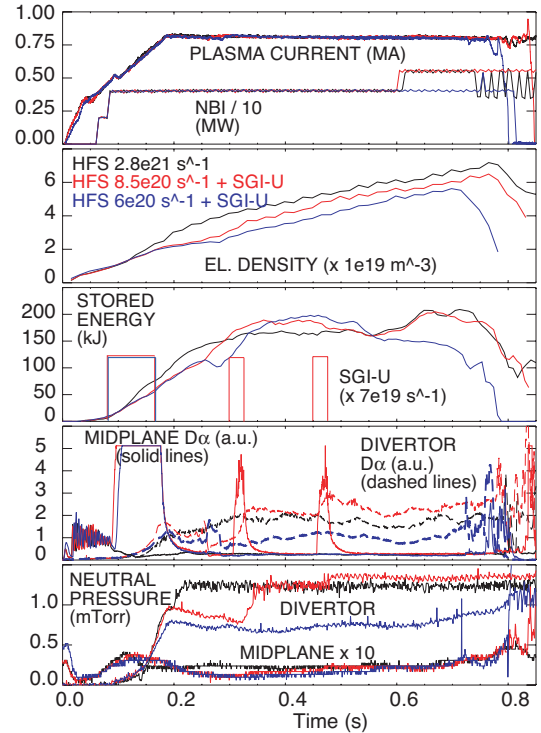


Figure 3: Waveforms of three H-mode discharges fueled by 1/ HFS injector only, 2/ reduced HFS injector rate and three SGI-U pulses, 3/ reduced HFS injector rate and one SGI-U pulse.

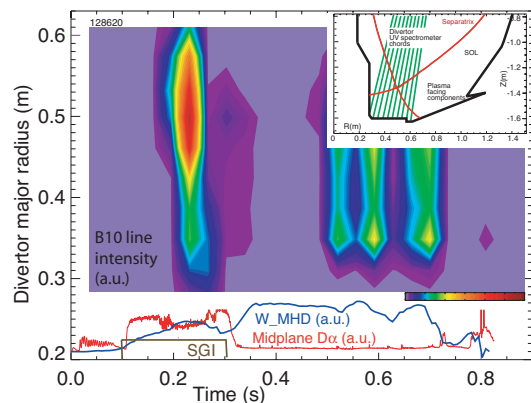


Figure 4: Spectroscopic evidence of X-point MARFE formation during SGI-U gas pulse.

Measured plasma background T_e and n_e profiles were used. A Maxwellian velocity distribution corresponding to a gas temperature of $T = 160$ K with a shift of $v = 2.4$ km/s was prescribed to the supersonic gas jet. Room temperature deuterium ($T = 300$ K) was used for the thermal GI. The SGI and GI fueling efficiencies η were found to be comparable, being in the range 0.35-0.39 for H-mode plasmas. In the simulations, the SGI molecular and ion source appeared to be highly localized. In contrast, a larger

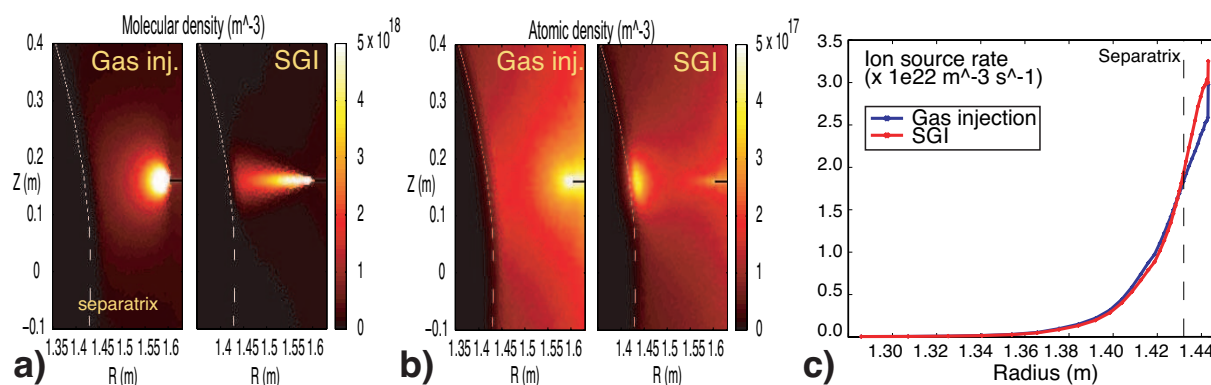


Figure 5: DEGAS 2 simulations of the conventional and supersonic gas injections in the H-mode plasmas: (a) molecular, (b) atomic densities, (c) flux surface averaged ionization rates. An artificial elongation 2:1 was given to panels (a) and (b) for clarity.

fraction of the GI molecules dissociated in the far SOL low temperature region, and the product Frank-Condon atoms were efficiently transported and ionized over a larger volume area. As a result, the flux-surface averaged η_{SGI} and η_{GI} were in the same range. Shown in Fig. 5 are the calculated molecular and atomic densities and the ion source rate for the SGI and GI cases. The simulations show that if the SGI operates in the "single-particle" regime, the directed velocity does not appear to lead to enhanced penetration or higher fueling efficiency.

In summary, recent H-mode experiments demonstrated that the high-pressure supersonic deuterium jet provides fast fueling control, high fueling efficiency, and reduced midplane neutral density. However, it appears that density control would not be possible in ELM-free or small ELM H-mode discharges without active pumping. The active pumping, to be provided in NSTX by lithium coatings, a liquid lithium divertor module, or a divertor cryopump, is expected to help mitigate the density rises and the impact of X-point MARFEs on core plasma confinement.

Acknowledgments We thank the entire NSTX Team for technical, computer and engineering support, as well as for plasma, NBI and diagnostic operations. This work is supported by U.S. DoE in part under contracts DE-AC52-07NA27344 and DE-AC02-76CH03073.

References

- [1] J. E. Menard et al. *Nucl. Fusion*, 47(10):645, 2007.
- [2] H. W. Kugel et al. *Phys. Plasmas*, 15:056118, 2008.
- [3] R. Kaita et al. Paper P1.009. In *Proc. this conference*, 2008.
- [4] V. A. Soukhanovskii et al. *Rev. Sci. Instrum.*, 75:4320, 2004.
- [5] V. A. Soukhanovskii et al. In *Proc. 21st IEEE/NPSS Symposium on Fus. Eng. (SOFE05)*, Knoxville, TN, Sep 26-29, 2005, IEEE.
- [6] Lianghua Yao et al. *Nucl. Fusion*, 41:817, 2001.
- [7] B. Pegourie et al. *J. Nuc. Mater.*, 313:539, 2003.
- [8] P. T. Lang et al. *Plasma Phys. Control. Fusion*, 47:1495, 2005.
- [9] V. Soukhanovskii et al. In *Proc. 31st EPS Conf. on Plasma Physics*, volume ECA 28G, page P2.190, London, UK, 2004.
- [10] V. Soukhanovskii et al. In *Proc. 33rd EPS Conf. on Plasma Physics*, volume ECA 30G, Rome, Italy, 2006.
- [11] V. A. Soukhanovskii et al. In *Proc. 22nd IEEE Symposium on Fus. Eng. (SOFE07)*, Albuquerque, NM, Jun 17-21, 2007, IEEE.
- [12] J. Yiming et al. *Plasma Phys. Control. Fusion*, 45:2001, 2003.
- [13] V. Rozhansky et al. *Nucl. Fusion*, 46(2):367, 2006.
- [14] R. Maingi et al. *Plasma Phys. Control. Fusion*, 46:A305, 2004.
- [15] V. A. Soukhanovskii et al. *J. Nuc. Mater.*, 337:475, 2005.
- [16] V. A. Soukhanovskii et al. *Rev. Sci. Instrum.*, 77:10F127, 2006.
- [17] D. P. Stotler et al. *Contrib. Plasma Phys.*, 44:3, 2004.